DOI: 10.1002/zaac.201300106

The Influence of OH Groups in $[Fe(CO)_3]_2[(\mu\text{-}ECH_2)_2C(CH_2OH)_2]$ (E = S, Se) Complexes toward the Cathodic Process

Ralf Trautwein,[a] Laith R. Almazahreh,[a] Helmar Görls,[a] and Wolfgang Weigand*[a,b]

Keywords: Iron; Hydrogenases; Hydrogen bonding; Electrochemistry; Selenium

Abstract. [FeFe] hydrogenase model complexes $[Fe(CO)_3]_2[(\mu\text{-}ECH_2)_2C(CH_2OH)_2]$ (E = S (**1**) or Se (**2**)) containing CH_2OH bridgehead substituents were synthesized via reaction of equimolar amounts of 4,4-bis(hydroxymethyl)-1,2-dithiolane (**A**) or 4,4-bis(hydroxymethyl)-1,2-diselenolane (**B**) with $Fe_3(CO)_{12}$ in toluene at 100 °C. The presence of OH groups in complexes **1** and **2** is found to influence the cathodic processes and their potentials. The catalytic reduction of acetic acid (AcOH) occurs by the anions $\mathbf{1}^-$ and $\mathbf{2}^-$, while the neutral complexes are procatalysts.

Introduction

Nature catalyzes the production of hydrogen with high efficiency and low energy features through [FeFe] hydrogenase showing a $[Fe_2S_3]$ cluster in its active site.[1–4] Inspired by these properties, there has been a great impetus to scientists for paving the way to design a cheap and robust electrocatalyst that mimics the structure of the active site. The activity of the enzyme in catalyzing the interconversion $2H^+ + 2e^- \leftrightarrow H_2$ is attributed to a structural feature, so called *rotated structure*, which offers a vacant site at the distal Fe_d^I in the reduced $\mathbf{H_{red}}$ and the oxidized $\mathbf{H_{ox}}$ states (Figure 1).[5] The catalytic formation of H_2 requires interaction of H^+ at the vacant site of $\mathbf{H_{red}}$ and the oxidation of dihydrogen occurs catalytically through binding at the vacant site of $\mathbf{H_{ox}}$. Thus, any successful synthetic model catalyst must possess a vacant coordination site or must be able to generate it during the catalytic cycle.

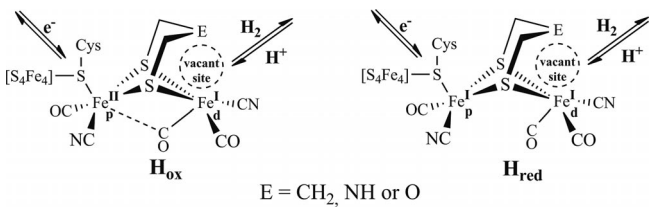

Figure 1. Structures of the active site in the $\mathbf{H_{ox}}$ and $\mathbf{H_{red}}$ states. Fe_d and Fe_p are distal and proximal iron atoms, respectively, with respect to the $[Fe_4S_4]$ cluster.

In all of the reported Fe^IFe^I complexes of the type $Fe_2(\mu\text{-}SR)_2(CO)_{6-n}L_n$ [L = PR_3, SR_2, CN^-, NCN (carbenes), n = 0–4], the CO ligands are in a terminal position. The rotated structure with bridging CO ligand has been detected for the reduced complexes with silicon[6], sulfur[7] and selenium[7] bridgehead atoms as well as for $[Fe(CO)_3]_2[(\mu\text{-1,2-benzenedithiolato})]$[8]. In addition, some oxidized complexes adopting the rotated structure are the nitrosyl-substituted diiron dithiolato complexes[10] and $\{[Fe(CO)_2PMe_3][Fe(CO)_2NHC][(\mu\text{-}SCH_2)_2CR_2)]\}^+$[8]. Moreover, the rotated structure has been calculated for the cationic species of the complexes containing sulfur[7] and selenium[7] bridgehead atoms as well as for $\{[Fe(CO)_3]_2[(\mu\text{-1,2-benzenedithiolato})]\}^+$[9]. In total picture, two factors, the steric and the electronic, are responsible for stabilizing the reduced and oxidized states: (*i*) The steric interaction between the bulky bridgehead groups and the apical CO lowers the rotational barrier of the $Fe(CO)_3$ moiety. (*ii*) Higher electron density at the iron atom due to strong electron donating groups such as PMe_3 and carbenes, respectively, favors the formation of a bridging CO ligand in the reduced and the oxidized forms, respectively.[11] The rotated structures of cationic complexes with sulfur or selenium bridgehead atoms are stabilized by the interaction between the lone pair of the bridgehead atom and the inverted iron atom. Additionally, the influence of H-bonding toward the stability of the reduced species has also been studied in $[Fe(CO)_3]_2[(\mu\text{-1,2-hydroquinonedithiolato})]$ and related structures.[12]

Herein, we describe the synthesis of the model complexes $[Fe(CO)_3]_2[(\mu\text{-}ECH_2)_2C(CH_2OH)_2]$ (E = S (**1**) or Se (**2**)). We discuss the influence of replacement of the alkyl bridgehead substituents in the complexes $[Fe(CO)_3]_2[(\mu\text{-}SCH_2)_2CR^1R^2]$ (R^1/R^2 = Me/Me, Et/Et, Bu/Et)[13] by CH_2OH in complexes **1** and **2** with respect to the mechanism of the cathodic process and the reduction potentials of the model complexes. Moreover, we study the electrochemical behavior of complexes **1** and **2** in the presence of acetic acid (AcOH) at various concentrations.

* Prof. Dr. W. Weigand
E-Mail: wolfgang.weigand@uni-jena.de
[a] Institut für Anorganische und Analytische Chemie
Friedrich-Schiller-Universität Jena
Humboldtstrasse 8
07743 Jena, Germany
[b] Jena Center for Soft Matter (JCSM)
Philosophenweg 7
07743 Jena, Germany

Supporting information for this article is available on the WWW under http://dx.doi.org/10.1002/zaac.201300106 or from the author.

Zeitschrift für anorganische und allgemeine Chemie ZAAC Journal of Inorganic and General Chemistry

Results and Discussion

Synthesis

Treatment of $Fe_3(CO)_{12}$ with compound **A**[14] or **B**[15] in toluene at 100 °C for one hour followed by column chromatography afforded complexes **1** and **2** in 45% and 41% yields, respectively (Scheme 1). We synthesized compound **A** according to Scheme 2.

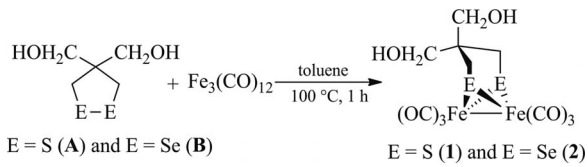

Scheme 1. Synthesis of complexes **1** and **2**.

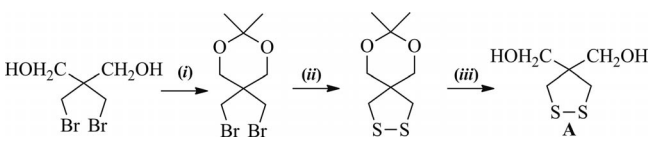

Scheme 2. Synthesis of compound **A**: (*i*) toluene/acetone, H_3PO_4, reflux, 16 h[15] (*ii*) EtOH, Na_2S_2, reflux, 4 h[14] (*iii*) EtOH/H_2O, HCl, room temperature, 24 h. The detailed procedure of step (*iii*) is presented in the Experimental Section.

Spectroscopic Characterization

Complexes **1** and **2** were characterized by ^1H, $^{13}C\{^1H\}$ and ^1H ^{77}Se HMBC (for complex **2**) NMR as well as IR spectroscopy, MS spectrometry, elemental analysis and X-ray crystallography. The MS spectra of complexes **1** and **2** reveal the parent ion peaks at m/z = 418 and 512 $[M - CO]^+$, respectively, and a stepwise fragmentation with the loss of five CO groups. In the IR spectrum of complex **1** (Figure S1 and S2), the CO absorptions bands (2072, 2022, 2001, 1985, 1980, 1961 cm^{-1}) are shifted to higher wavenumbers compared to those of complex **2** (2062, 2013, 1993, 1972, 1968, 1951 cm^{-1}) (Figures S3 and S4). These shifts indicate increased electron density at the diiron core when sulfur is replaced by selenium being consistent with the different electronegativities.[7,16] The ^1H NMR spectrum of complex **1** exhibits a singlet at δ = 2.38 ppm due to the CH_2S protons, a doublet centered at δ = 3.39 ppm for the CH_2O ($^3J_{H,H}$ = 4.9 Hz) and a triplet centered at δ = 4.05 ppm owing to the OH protons ($^3J_{H,H}$ = 5.2 Hz). In the ^1H NMR spectrum of complex **2**, the protons of CH_2S, CH_2O and OH resonate at 2.44 (singlet with ^{77}Se satellites, $^2J_{Se,H}$ = 19.0 Hz), 3.40 (doublet with $^3J_{H,H}$ = 4.8 Hz) and 4.04 (triplet with $^3J_{H,H}$ = 5.0 Hz) ppm, respectively. The $^{13}C\{^1H\}$ NMR spectrum of complex **1** shows four singlets at 23.4, 43.5, 65.3 and 208.9 ppm attributing to the carbon atoms of CH_2S, the quaternary bridgehead atom, CH_2O and the carbonyl carbon atoms, respectively. In the $^{13}C\{^1H\}$ NMR spectrum of complex **2**, the carbon atoms of the CH_2Se groups resonate at δ = 16.2 ppm as singlet with ^{77}Se satellites, ($^1J_{Se,C}$ = 83 Hz). The spectrum shows also a singlet at δ = 42.8 ppm for the bridgehead carbon atom and additional signals for the carbon atoms of the CH_2O and $Fe(CO)_3$ moieties at 64.6 and 209.7 ppm, respectively. The ^1H ^{77}Se HMBC NMR spectrum of complex **2** displays a singlet at δ = 74.5 ppm for the selenium atoms.

Molecular Structures

Single crystals suitable for X-ray diffraction studies were obtained by diffusion of pentane into a concentrated benzene solution of complex **1** or **2** at room temperature. Molecular structures and numbering schemes of the complexes are shown in Figure 2. As can be seen in Figure 2, each iron center in **1** or **2** adopts a distorted octahedral geometry with three *facial* CO ligands, one iron atom and two bridging sulfur atoms with *cis*-fashion. The bicyclic $[Fe_2S_2]$ structure in these complexes reveals butterfly conformation. The bridgehead carbon atom is surrounded in a distorted tetrahedral environment.

The Fe–Fe bond length in complex **1** [2.5006(5) Å] is shorter than that in complex **2** [2.5473(7) Å] because of the smaller size of sulfur compared to that of selenium.[7,17] The Fe–Fe bond lengths in both complexes are shorter than those of the active site, 2.55–2.62 Å[18], but within the range of the previously reported model complexes. Interestingly, the average C–C–S angle in complex **1** (121.1°) and the average C–C–Se angle in complex **2** (121.7°) are larger than those found in model complexes with carbon bridgehead atoms[19], but comparable to those in complexes containing silicon and tin bridgehead heteroatoms[6,20]. The molecular packings of

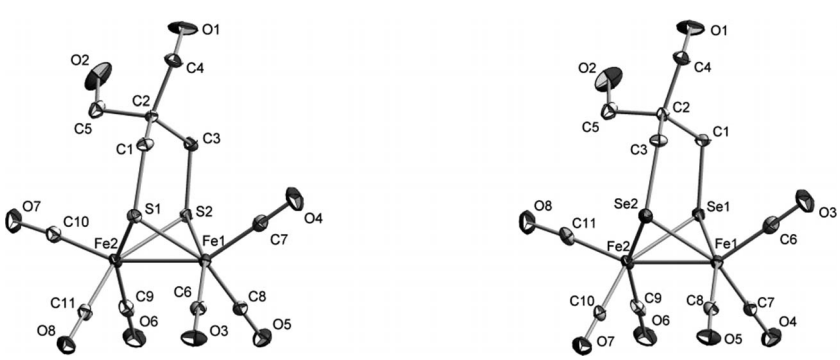

Figure 2. Molecular structures (50% probability) of complexes **1** (left) and **2** (right). Hydrogen atoms were omitted for clarity.

Special Issue

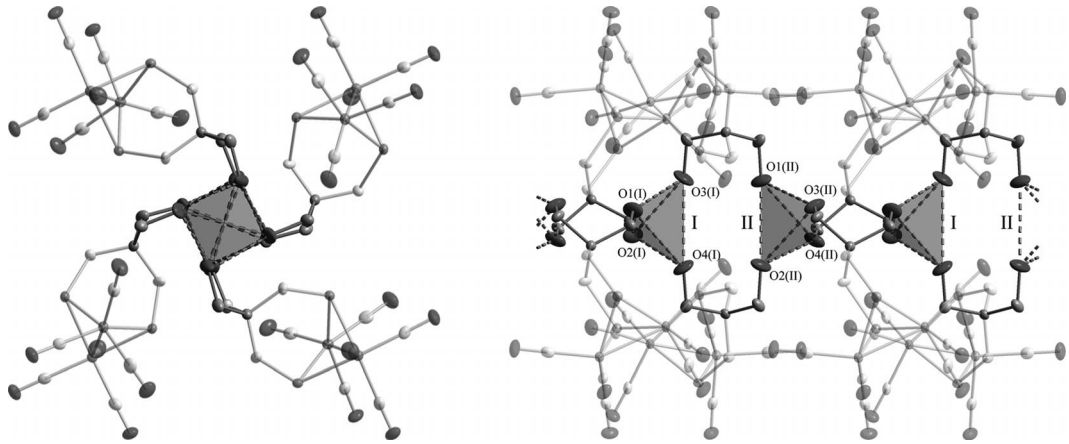

Figure 3. Molecular packing of **2**. Hydrogen atoms were omitted for clarity. Left: View along the axis of the $[OH]_4$ tetrahedra. Right: Rotated by 90°. Linear arrangement of two different distorted $[OH]_4$ tetrahedra I and II in alternating order. Tetrahedron I: $d_{O\cdots O}$ = 3.19 and 2.85 Å; tetrahedron II: $d_{O\cdots O}$ = 3.11 and 2.87 Å.

compounds **1** (Figure S5) and **2** (Figure 3) show strains of the two alternating distorted $[OH]_4$ tetrahedra I and II. Within one tetrahedron we observe four shorter O···O and two longer O···O distances. The molecular packing of compound **B** displays an intermolecular hydrogen bonding system with slightly shorter O···O distances (2.69 Å) compared to those in compound **2**.[15] Similar packing structures via intermolecular hydrogen bonding can be observed for $[Fe(CO)_3]_2[(\mu\text{-}SCH_2)_2CHOH]$ and the carboxylic acid functionalized model $[Fe(CO)_3]_2[(\mu\text{-}SCH_2)_2CHCOOH]$.[21] Furthermore, intermolecular hydrogen bonding involving nitrogen atoms are described in some model complexes containing amino acid derivatives as ligands.[22]

In contrast to $[Fe(CO)_3]_2[(\mu\text{-}SCH_2)_2CH_2]$[23], complexes **1** and **2** exhibit torsion angles defined by the apical CO across the Fe–Fe bond (OC_{ap}–Fe–Fe–CO_{ap}) due to the presence of sterically demanding CH_2OH substituents at the bridgehead atoms. The torsion angle in complex **2** (11.2°) is larger than that in complex **1** (8.2°), whereas the basal CO groups in both complexes are almost eclipsed (see Figure 4). The influence of the steric demand of the bridgehead toward the solid-state structure of the $Fe_2S_2(CO)_6$ moiety has also been described in $[Fe(CO)_3]_2[(\mu\text{-}SCH_2)_2CR^1R^2]$ (R^1/R^2 = Me/Me, Et/Et), where the apical CO torsion angles are 6° (R^1/R^2 = Me/Me) and 15.8° (R^1/R^2 = Et/Et).[13] The smaller torsion angle in complexes **1** and **2** compared to that in $[Fe(CO)_3]_2[(\mu\text{-}SCH_2)_2CEt_2]$ is due to the less steric bulk of the CH_2OH compared to the Et substituents.

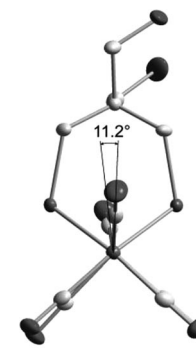

Figure 4. Torsion angle (OC_{ap}–Fe–Fe–CO_{ap}) in complex **2**. Hydrogen atoms were omitted for clarity.

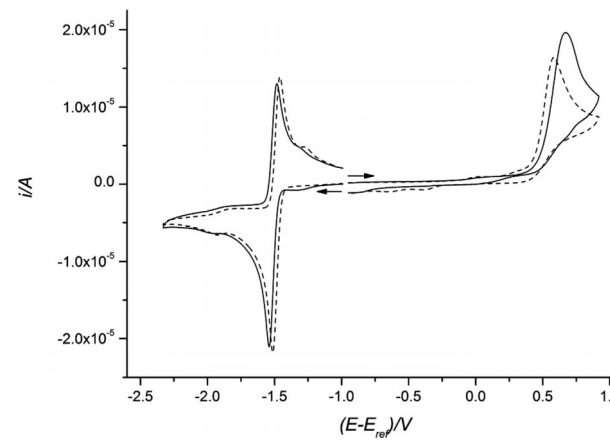

Figure 5. CVs. of complexes 1 (solid line) and 2 (dashed line) measured at 200 mV·s^{-1} scan rate. The concentration of the complexes is 1.0 mM.

Electrochemical Properties in Absence of Acid

Cyclic voltammograms (CVs.) of complexes **1** and **2** are shown in Figure 5. Complexes **1** and **2** exhibit reversible cathodic peaks at $E_{1/2}$ = –1.53 V and –1.49 V (vs. Fc/Fc^+), respectively. An additional reduction event (**1**: –1.97, **2**: –1.93 V) can be seen at a potential more negative than that for the primary reduction of the complexes. The oxidative parts of the CVs. show irreversible oxidation events at +0.67 V and +0.58 V for complexes **1** and **2**, respectively.

At a scan rate of 200 mV·s^{-1} the primary cathodic waves of **1** and **2** are assigned to two successive reduction steps, *RS1*

Zeitschrift für anorganische und allgemeine Chemie ZAAC Journal of Inorganic and General Chemistry

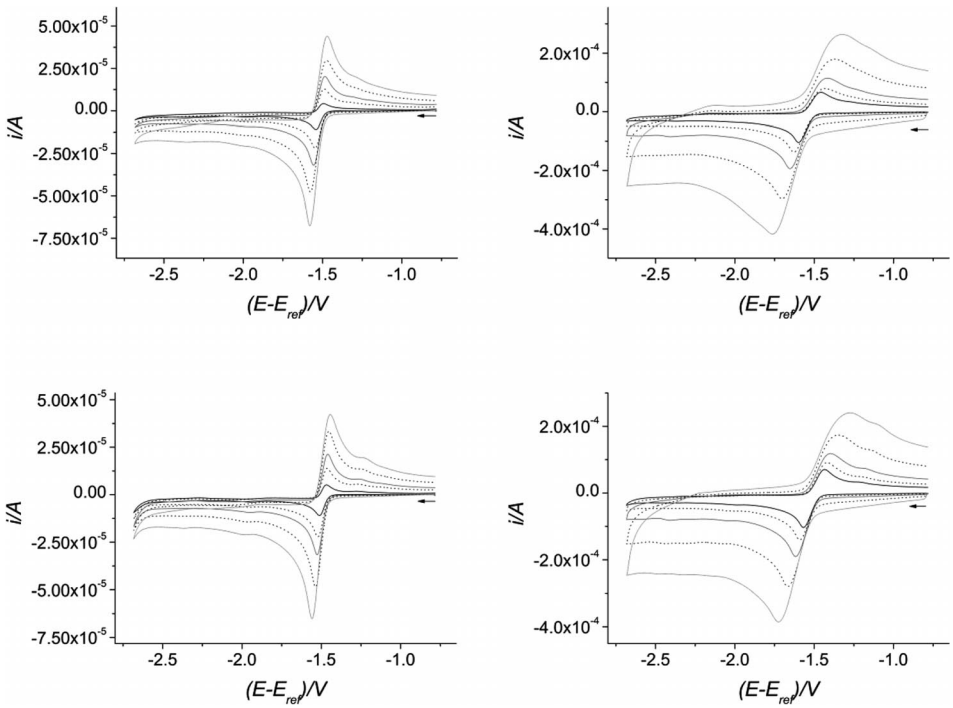

Figure 6. CVs. of complex **1** at 0.05, 0.2, 0.4, 1 and 2 V•s^{-1} (top left), **1** at 5, 10, 20, 50 and 100 V•s^{-1} (top right), **2** a 0.05, 0.2, 0.4, 1 and 2 V•s^{-1} (bottom left) and **2** at 5, 10, 20, 50 and 100 V•s^{-1} (bottom right).

and *RS2*, with closely spaced individual standard reduction potentials, $E°_1$ and $E°_2$, respectively.

$Fe^IFe^I + e^- \leftrightarrow Fe^IFe^0$ ($E°_1$, k_s^1) (RS1)

$Fe^IFe^0 + e^- \leftrightarrow Fe^0Fe^0$ ($E°_2$, k_s^2) (RS2)

The kinetic parameters k_s^1 and k_s^2 are the heterogeneous electron transfer rate constants for *RS1* and *RS2*, respectively. Thus, the reduction events at –1.97 V and –1.93 V for complex **1** and **2**, respectively, should be due to daughter products of follow-up reactions. It is likely that these chemical reactions involve CO loss either from the anion or the dianion as it was found for various diiron carbonyl complexes.[23,24] The anodic waves at +0.67 V and +0.58 V for complexes **1** and **2**, respectively, are assigned to the oxidation of Fe^IFe^I to $Fe^{II}Fe^{II}$. The conclusion that the primary cathodic waves of complexes **1** and **2** correspond to both *RS1* and *RS2* is based on comparison of the peak height with that of $[Fe(CO)_3]_2[(\mu\text{-}SCH_2)_2CH_2]$, which is closer to a one electron process at 200 mV•s^{-1} scan rate:[8,25] The peak heights of the cathodic waves of complexes **1** and **2** are almost twice the peak height of $[Fe(CO)_3]_2[(\mu\text{-}SCH_2)_2CH_2]$ under the same conditions (Figures S6 and S7). In addition, the intensity of these reduction waves increases at faster scan rates up to 100 V•s^{-1}, while the events at more negative potentials become less visible (Figure 6). By increasing the scan rate wave-splitting is not observed for the primary reduction of complexes **1** and **2** even at 100 V•s^{-1} scan rate which implies that the second heterogeneous rate constant k_s^2 is larger than, or similar to k_s^1.[24i,26]

The question that arises now is: *Why does the cathodic process of complexes **1** and **2** tend to be two-electron reduction even at fast scan rates?* Typically, chemical reactions accompanying the electron-transfer processes result in stabilizing the SOMO to a level comparable or lower than the Fermi level of the electrode being necessary for the first electron-transfer process. The second electron transfer from the electrode to the stabilized SOMO will occur at the Fermi level required for the first electron transfer to the LUMO of the neutral species. Stated simply, two-electron cathodic wave is observed when a structural change makes the transfer of a second electron thermodynamically more favorable than, or comparable to the first. The structural change, as it has been found for various complexes of the type $[Fe(CO)_3]_2[(\mu\text{-}ECH_2)_2X]$ (E = S, Se; X = bridgehead group), includes: (*i*) elongation of the Fe–Fe bond, (*ii*) cleavage of one of the Fe–E bonds and (*iii*) rotation of one $Fe(CO)_3$ unit to allow orientation of one of its CO ligands into bridging or semi-bridging position to delocalize the negative charge.[6–8,24i] Previous DFT calculations showed that the structural change can occur mainly on the anion[7,27] or on the dianion[24i]. The described rearrangements result in a rotated structure with an open site, which is similar to the active site in $\mathbf{H_{red}}$ state (Figure 7). Consequently, the two-electron nature of the reduction waves of complexes **1** and **2** can be explained by structural rearrangements most likely leading to a structure similar to that depicted in Figure 7. However, the cathodic processes of the structural analogues $[Fe(CO)_3]_2[(\mu\text{-}SCH_2)_2CR^1R^2]$ (R^1/R^2 = Me/Me, Et/Et, Bu/Et) of complexes **1** and **2** show two one-electron reduction waves: a quasi-reversible event at approx. –1.6 V and an irreversible reduction at approx. –2.4 V (for R^1/R^2 = Et/Et).[13] In other words, replacement of the alkyl bridgehead substituents in these com-

Special Issue

plexes by CH_2OH as in complexes **1** and **2** results in altering the cathodic process from one- into two-electron transfer. Clearly, these findings reveal the influence of OH toward the reduction mechanism.

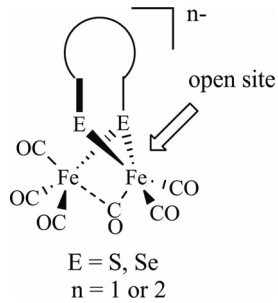

Figure 7. Proposed rotated structure of the reduced species obtained by reduction of the neutral complex.

It has been reported that the model complex $[Fe(CO)_3]_2[(\mu$-1,2-hydroquinonedithiolato)] and related structures were stabilized in the neutral and the reduced forms via internal hydrogen bonding between the OH groups and the adjacent sulfur atoms.[12] However, this study does not show whether the presence of hydrogen bonding can switch the cathodic process from one- into two-electron transfer or not, because the complex $[Fe(CO)_3]_2[(\mu$-1,2-hydroquinonedithiolato)] and the unsubstituted $[Fe(CO)_3]_2[(\mu$-1,2-benzenedithiolato)] exhibit a two-electron cathodic wave. In the light of these findings, we suggested that the driving force for rotated structure formation upon reduction of complex **1** or **2** can be due to the hydrogen bonding between the OH group and the inverted iron or the chalcogen atom as shown in Figure 8. The hydrogen bondings may also account for the less negative reduction potentials of complexes **1** and **2** compared to $[Fe(CO)_3]_2[(\mu\text{-}SCH_2)_2CR^1R^2]$ (R^1/R^2 = Me/Me, Et/Et, Bu/Et).

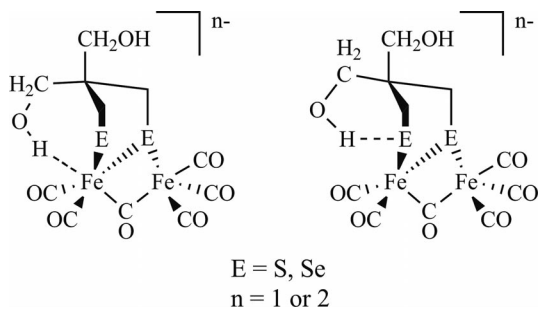

Figure 8. Proposed hydrogen bonding in the reduced complexes **1** and **2**.

Electrocatalytic Proton Reduction

CVs. of complexes **1** and **2** in the presence of AcOH at different concentrations show no increase in the current of the two-electron cathodic waves, but suppression of the anodic waves for the oxidation of the dianions. However, the catalytic proton reduction waves are observed near –1.8 V and –1.9 V for complexes **1** and **2**, respectively (Figure 9). In case of complex **2**, it seems that there are two catalytic processes, process *I* and process *II*, as shown in Figure 9. The catalytic current of process *II* increases faster than that of process *I*, which cannot be observed clearly at higher AcOH concentrations. Nevertheless, it is not the main task of our current study to investigate these mechanistic details of acid reduction in case of complex **2**.

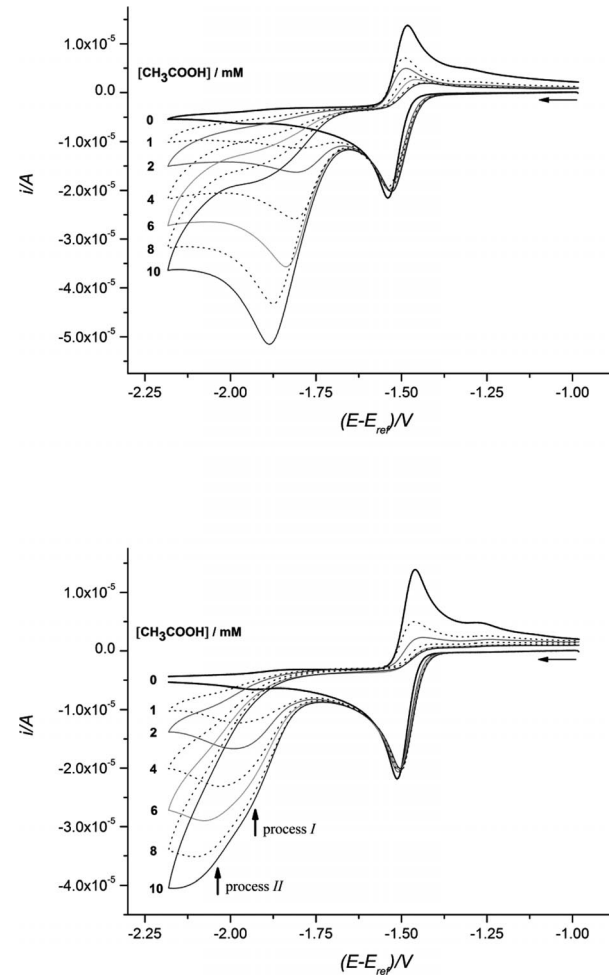

Figure 9. CVs. of complexes **1** (1.0 mM) (top) and **2** (1.0 mM) (bottom) at various concentrations of AcOH.

Indeed, this catalytic reduction of AcOH by complex **1** is similar to other systems, which show two-electron cathodic waves in the absence of acid.[7,27] A detailed catalytic mechanism of AcOH reduction has been described for $[Fe(CO)_3]_2[(\mu$-bdt)] (bdt = benzenedithiolato) as ECEC.[27] Therefore, we explain the catalytic reduction of AcOH by complex **1** through ECEC mechanism in which the catalyst is the anion $\mathbf{1}^-$ (Scheme 3).

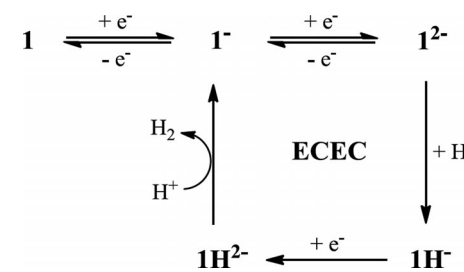

Scheme 3. Proposed ECEC mechanism for electrocatalytic reduction of AcOH by complex **1**.

Zeitschrift für anorganische und allgemeine Chemie ZAAC Journal of Inorganic and General Chemistry

Conclusions

Model complexes **1** and **2** have been synthesized and characterized by ^{1}H, ^{13}C{^{1}H} and ^{1}H ^{77}Se HMBC NMR as well as IR spectroscopy, mass spectrometry, elemental analysis and X-ray crystallography. The presence of sterically demanding groups at the bridgehead of the complexes results in torsion angle defined by the apical CO across the Fe–Fe bond. Replacement of the alkyl substituents in $[Fe(CO)_3]_2[(\mu\text{-}SCH_2)_2CR^1R^2]$ (R^1/R^2 = Me/Me, Et/Et, Bu/Et)[13] by CH_2OH substituents in complexes **1** and **2** alters the cathodic process from one- into two-electron transfer. Moreover, the replacement of the alkyl groups by CH_2OH leads to lowering the reduction potentials. To explain these observations, we assume that structural change occurs during the cathodic process leading to a *rotated structure*, which involves internal hydrogen bonding between the OH group and the iron or the sulfur atom. The anions $\mathbf{1}^-$ and $\mathbf{2}^-$ are the actual catalysts for the reduction of AcOH. The substitution of sulfur by selenium in our complexes results in a longer Fe–Fe bond, smaller CO wavenumbers and a higher overpotential concerning the catalytic reduction of AcOH.

Experimental Section

All reactions were performed using standard Schlenk and vacuum-line techniques under N_2 atmosphere. The ^{1}H, ^{13}C{^{1}H}, and ^{1}H ^{77}Se HMBC NMR spectra were recorded with Bruker Avance 200 MHz or 400 MHz spectrometer. Chemical shifts are given in parts per million with reference to $SiMe_4$ (^{1}H, ^{13}C) or to Me_2Se (^{1}H ^{77}Se HMBC). Mass spectra were recorded with a Finnigan MAT SSQ 710 instrument. FTIR spectra were recorded with a Bruker Equinox 55 spectrometer equipped with an ATR unit. Elemental analysis was performed with a Leco CHNS-932 apparatus. Silica gel 60 (0.015–0.040 mm) was used for column chromatography and TLC was performed using Merck TLC aluminum sheets (Silica gel 60 F254). Chemicals were purchased from Fisher Scientific, Aldrich or Acros and were used without further purification. All solvents were dried and distilled prior to use according to standard methods. The starting material **B**[15] was prepared according to literature procedures.

Electrochemistry

Cyclic voltammetric measurements were conducted in three-electrode technique [glassy carbon disk (diameter = 1.6 mm), the working electrode; reference electrode, Ag/AgCl in CH_3CN; and a platinum wire, the counter electrode] using a Reference 600 Potentiostat (Gamry Instruments). All experiments were performed in CH_3CN solutions containing 0.1 M Bu_4NBF_4 at room temperature. The solutions were purged with N_2 for five minutes and a stream of N_2 was maintained over the solutions during the measurements. All potential values reported in this paper are referenced to the potential of the Fc/Fc^+ couple.

Crystal Structure Determination of Complexes 1 and 2

The intensity data were collected on a Nonius KappaCCD diffractometer, using graphite-monochromated Mo-K_α radiation. Data were corrected for Lorentz and polarization effects, but not for absorption.[28,29].The structure was solved by direct methods (SHELXS[30]) and refined by full-matrix least square techniques against F_o^2 (SHELXL-97[30]). All hydrogen atoms were included at calculated positions with fixed thermal parameters. All non-hydrogen atoms were refined anisotropically.[30] XP (SIEMENS Analytical X-ray Instruments, Inc.) was used for structure representations.

***Crystal data for complex* 1**: $C_{11}H_{10}Fe_2O_8S_2$, M_r = 446.012 g·mol^{-1}, red-brown prism, size 0.06 × 0.03 × 0.03 mm, tetragonal, space group $I4_1/a$, a = 26.5730(4), b = 26.5730(4), c = 8.8956(1) Å, V = 6281.40(15) Å^3, T = –140 °C, Z = 16, $\rho_{calcd.}$ = 1.887 g·cm^{-3}, μ(Mo-K_α) = 21.49 cm^{-1}, F(000) = 3584, 18960 reflections in h(–34/34), k(–34/25), l(–11/11), measured in the range 2.41° ≤ Θ ≤ 27.48°, completeness Θ_{max} = 99.9 %, 3602 independent reflections, R_{int} = 0.0435, 3295 reflections with $F_o > 4\sigma(F_o)$, 208 parameters, 0 restraints, R^1_{obs} = 0.0356, wR^2_{obs} = 0.0670, R^1_{all} = 0.0414, wR^2_{all} = 0.0688, GOOF = 1.182, largest difference peak and hole: 0.594 / –0.433 e·Å^{-3}.

***Crystal data for complex* 2**: $C_{11}H_{10}Fe_2O_8Se_2$, M_r = 539.802 g·mol^{-1}, brown prism, size 0.06 × 0.06 × 0.06 mm, tetragonal, space group $I4_1/a$, a = 26.9243(4), b = 26.9243(4), c = 8.9234(1) Å, V = 6468.73(15) Å^3, T = –140 °C, Z = 16, $\rho_{calcd.}$ = 2.217 g·cm^{-3}, μ (Mo-K_α) = 63.3 cm^{-1}, F(000) = 4160, 18984 reflections in h(–34/24), k(–34/30), l(–11/11), measured in the range 2.40° ≤ Θ ≤ 27.48°, completeness Θ_{max} = 99.8 %, 3711 independent reflections, R_{int} = 0.0392, 3394 reflections with $F_o > 4\sigma(F_o)$, 210 parameters, 0 restraints, R^1_{obs} = 0.0315, wR^2_{obs} = 0.0590, R^1_{all} = 0.0373, wR^2_{all} = 0.0610, GOOF = 1.255, largest difference peak and hole: 0.526 / –0.573 e·Å^{-3}.

Synthesis of A [step (iii) in Scheme 2]

To a stirred solution of crude 8,8-dimethyl-7,9-dioxa-2,3-dithiaspiro-[4.5]decan prepared from (2.00 g, 6.62 mmol) 5,5-bis(bromomethyl)-2,2-dimethyl-1,3-dioxane in ethanol/water (30 mL/20 mL) was added concentrated hydrochloric acid (1 mL). After stirring overnight at room temperature most of the solvent was removed under reduced pressure and the remaining aqueous phase was extracted five times with dichloromethane. The combined organic phases were washed with water, dried with sodium sulfate and the solvents evaporated to dryness. Crystallization from chloroform gave **A** (0.56 g, 3.37 mmol) in 52 % yield as slight yellow crystals. **^{1}H NMR** (400 MHz, [D$_6$]DMSO, 24 °C): δ = 4.88 (t, $^3J_{H,H}$ = 5.4 Hz, 2 H, O*H*), 3.41 (d, $^3J_{H,H}$ = 5.2 Hz, 4 H, C*H*$_2$OH), 2.90 (s, 4 H, SC*H*$_2$). **^{13}C{^{1}H} NMR** (101 MHz, [D$_6$]DMSO, 24 °C): δ = 62.96 (s, *C*H$_2$OH), 58.69 (s, *C*CH$_2$), 43.68 (s, S*C*H$_2$). **EI-MS:** m/z = 166 [M]$^+$. $C_5H_{10}O_2S_2$ (166.262 g·mol^{-1}): C 36.15 (calcd. 36.12), H 6.06 (6.06), S 37.27 (38.57)%.

General Procedure for the Synthesis of Complexes 1 and 2

Equimolar amounts of $Fe_3(CO)_{12}$ and either **A** or **B** were suspended in toluene under N_2 atmosphere and the resulting green suspension was stirred for 1 h at 100 °C resulting in a color change to reddish brown. After removal of the solvent under vacuum, the solid residue was purified by column chromatography (dichloromethane/acetone 10/1) to afford complexes **1** and **2** as red and reddish brown solids, respectively.

Complex 1: A (280 mg, 1.684 mmol) and $Fe_3(CO)_{12}$ (848 mg, 1.684 mmol) in toluene (20 mL): 340 mg, 45 %. **^{1}H NMR** (200 MHz, [D$_6$]acetone, 23 °C): δ = 4.05 (t, $^3J_{H,H}$ = 5.2 Hz, 2 H, O*H*), 3.39 (d, $^3J_{H,H}$ = 4.9 Hz, 4 H, C*H*$_2$OH), 2.38 (s, 4 H, SC*H*$_2$). **^{13}C{^{1}H} NMR**

Special Issue

(50 MHz, [D_6]acetone, 22 °C): δ = 208.85 (s, *C*O), 65.29 (s, *C*H_2OH), 43.51 (s, *C*CH_2), 23.44 (s, S*C*H_2). **IR:** 3278 (υ_{OH}), 2072 (υ_{CO}), 2022 (υ_{CO}), 2001 (υ_{CO}), 1985 (υ_{CO}), 1980 (υ_{CO}), 1961 (υ_{CO}), 1075, 1025, 615, 561, 503 cm^{-1}. **DEI-MS:** *m/z* = 418 $[M–CO]^+$, 390 $[M–2CO]^+$, 362 $[M–3CO]^+$, 336 $[M–4CO]^+$, 306 $[M–5CO]^+$, 278 $[M–6CO]^+$. $C_{11}H_{10}Fe_2O_8S_2$ (446.012 g·mol^{-1}): C 29.76 (calcd. 29.62), H 2.39 (2.26), S 14.60 (14.38)%.

Complex 2: B (110 mg, 0.423 mmol) and $Fe_3(CO)_{12}$ (213 mg, 0.423 mmol) in toluene (10 mL): 93 mg, 41 %. **^{1}H NMR** (400 MHz, [D_6]acetone, 27 °C): δ = 4.04 (t, $^3J_{H,H}$ = 5.0 Hz, 2 H, O*H*), 3.40 (d, $^3J_{H,H}$ = 4.8 Hz, 4 H, C*H*$_2$OH), 2.44 (s with ^{77}Se satellites, $^2J_{Se,H}$ = 19.0 Hz, 4 H, SeC*H*$_2$). **^{13}C{^{1}H} NMR** (101 MHz, [D_6]acetone, 24 °C): δ = 209.71 (s, *C*O), 64.61 (s, *C*H_2OH), 42.80 (s, *C*CH_2), 16.21 (s with ^{77}Se satellites, $^1J_{Se,C}$ = 83 Hz, Se*C*H_2). **^{1}H ^{77}Se HMBC NMR** (400 MHz/76 MHz, [D_6]acetone, 24 °C): δ = 74.51 (s, *Se*CH_2). **IR:** 3307 (υ_{OH}), 2062 (υ_{CO}), 2013 (υ_{CO}), 1993 (υ_{CO}), 1972 (υ_{CO}), 1968 (υ_{CO}), 1951 (υ_{CO}), 1075, 1025, 615, 561, 503 cm^{-1}. **DEI-MS:** *m/z* = 512 $[M–CO]^+$, 484 $[M–2CO]^+$, 456 $[M–3CO]^+$, 428 $[M–4CO]^+$, 400 $[M–5CO]^+$, 372 $[M–6CO]^+$. $C_{11}H_{10}Fe_2O_8Se_2$ (539.802 g·mol^{-1}) ·0.25C_3H_6O: C 25.38 (calcd. 25.46), H 2.15 (2.09)%.

Crystallographic data (excluding structure factors) have been deposited with the Cambridge Crystallographic Data Centre as supplementary publication CCDC-925461 for **1** and CCDC-925462 for **2**. Copies of the data can be obtained free of charge on application to CCDC, 12 Union Road, Cambridge CB2 1EZ, UK [E-mail: deposit@ccdc.cam.ac.uk].

Supporting Information (see footnote on the first page of this article): IR spectra of complexes **1** and **2**, additional cyclovoltammetric data, molecular packing of **1** as well as depicted distances in the molecular packing of **1** are shown in the Supporting Information.

Acknowledgments

L. A. thanks the Deutscher Akademischer Austausch Dienst (DAAD) for scholarship. We are thankful to *David Hornig* for IR spectroscopic investigations and *Prof. Christian Robl* for discussion.

References

[1] a) M. Frey, *ChemBioChem* **2002**, *3*, 153–160; b) R. Cammack, *Nature* **1999**, *397*, 214–215; c) P. M. Vignais, B. Billoud, *Chem. Rev.* **2007**, *107*, 4206–4272; d) J. C. Fontecilla-Camps, A. Volbeda, C. Cavazza, Y. Nicolet, *Chem. Rev.* **2007**, *107*, 4273–4303; e) A. L. De Lacey, V. M. Fernandez, M. Rousset, R. Cammack, *Chem. Rev.* **2007**, *107*, 4304–4330.

[2] Y. Nicolet, C. Piras, P. Legrand, C. E. Hatchikian, J. C. Fontecilla-Camps, *Structure* **1999**, *7*,13–23.

[3] J. W. Peters, W. N. Lanzilotta, B. J. Lemon, L. C. Seefeldt, *Science* **1998**, *282*, 1853–1858.

[4] a) C. Tard, C. Pickett, *Chem. Rev.* **2009**, *109*, 2245–2274; b) S. Roy, S. Shinde, G. A. Hamilton, H. E. Hartnett, A. K. Jones, *Eur. J. Inorg. Chem.* **2011**, 1050–1055; b) W. Gao, L.-C. Song, B.-S. Yin, H.-N. Zan, D.-F. Wang, H.-B. Song, *Organometallics* **2011**, *30*, 4097–4107; c) G. Durgaprasad, R. Bolligarla, S. K. Das, *J. Organomet. Chem.* **2012**, *706–707*, 37–45; d) C. Topf, U. Monkowius, G. Knör, *Inorg. Chem. Commun.* **2012**, *21*, 147–150.

[5] a) Y. Nicolet, A. L. de Lacey, X. Vernede, V. M. Fernandez, E. C. Hatchikian, J. C. Fontecilla-Camps, *J. Am. Chem. Soc.* **2001**, *123*, 1596–1601; b) Y. Nicolet, B. J. Lemon, J. C. Fontecilla-Camps, J. W. Peters, *Trends Biochem. Sci.* **2000**, *25*, 138–143.

[6] a) U.-P. Apfel, D. Troegel, Y. Halpin, S. Tschierlei, U. Uhlemann, H. Görls, M. Schmitt, J. Popp, P. Dunne, M. Venkatesan Coey, M. Rudolph, G. J. Vos, R. Tacke, W. Weigand, *Inorg. Chem.* **2010**, *49*, 10117–10132; b) U.-P. Apfel, Y. Halpin, H. Görls, G. J. Vos, W. Weigand, *Eur. J. Inorg. Chem.* **2011**, 581–588; c) U.-P. Apfel, H. Görls, G. A. N. Felton, D. H. Evans, R. S. Glass, D. L. Lichtenberger, W. Weigand, *Helv. Chim. Acta* **2012**, *95*, 2168–2175.

[7] M. K. Harb, J. Windhager, T. Niksch, H. Görls, T. Sakamoto, E. R. Smith, R. S. Glass, D. L. Lichtenberger, D. H. Evans, M. El-khateeb, W. Weigand, *Tetrahedron* **2012**, *68*, 10592–10599.

[8] T. Liu, M. Y. Darensbourg, *J. Am. Chem. Soc.* **2007**, *129*, 7008–7009.

[9] J. S. McKennis, E. P. Kyba, *Organometallics* **1983**, *2*, 1249–1251.

[10] a) W. Ziegler, H. Umland, U. Behrens, *J. Organomet. Chem.* **1988**, *344*, 235–247; b) M. T. Olsen, M. Bruschi, L. De Gioia, T. B. Rauchfuss, S. R. Wilson, *J. Am. Chem. Soc.* **2008**, *130*, 12021–12030; c) C.-H. Hsieh, Ö. F. Erdem, S. D. Harman, M. L. Singleton, E. Reijerse, W. Lubitz, C. V. Popescu, J. H. Reibenspies, S. M. Brothers, M. B. Hall, M. Y. Darensbourg, *J. Am. Chem. Soc.* **2012**, *134*, 13089–13102.

[11] I. P. Georgakaki, L. M. Thomson, E. J. Lyon, M. B. Hall, M. Y. Darensbourg, *Coord. Chem. Rev.* **2003**, *255*, 238–239.

[12] J. Chen, A. K. Vannucci, C. A. Mebi, N. Okumura, S. C. Borowski, M. Swenson, L. Tori Lockett, D. H. Evans, R. S. Glass, D. L. Lichtenberger, *Organometallics* **2010**, *29*, 5330–5340.

[13] M. L. Singleton, R. M. Jenkins, C. L. Klemashevich, M. Y. Darensbourg, *C. R. Chim.* **2008**, *11*, 861–874.

[14] R. Gropeanu, M. Tintas, C. Pilon, M. Morin, L. Breau, R. Turdean, I. Grosu, *J. Heterocycl. Chem.* **2007**, *44*, 521–527.

[15] T. Niksch, H. Görls, M. Friedrich, R. Oilunkaniemi, R. Laitinen, W. Weigand, *Eur. J. Inorg. Chem.* **2010**, 74–94.

[16] M. K. Harb, T. Niksch, J. Windhager, H. Görls, R. Holze, L. T. Lockett, N. Okumura, D. H. Evans, R. S. Glass, D. L. Lichtenberger, M. El-khateeb, W. Weigand, *Organometallics* **2009**, *28*, 1039–1048.

[17] a) M. K. Harb, U.-P. Apfel, J. Kübel, H. Görls, G. A. N. Felton, T. Sakamoto, D. H. Evans, R. S. Glass, D. L. Lichtenberger, M. El-khateeb, W. Weigand, *Organometallics* **2009**, *28*, 6666–6675; b) L.-C. Song, B. Gai, H.-T. Wang, Q.-M. Hu, *J. Inorg. Biochem.* **2009**, *103*, 805–812.

[18] a) Y. Nicolet, C. Piras, P. Legrand, C. E. Hatchikian, J. C. Fontecilla-Camps, *Structure* **1999**, *7*, 13–23; b) J. W. Peters, W. N. Lanzilotta, B. J. Lemon, L. C. Seefeldt, *Science* **1998**, *282*, 1853–1858; c) Y. Nicolet, A. L. Lacey, X. Vernède, V. M. Fernandez, E. C. Hatchikian, J. C. Fontecilla-Camps, *J. Am. Chem. Soc.* **2001**, *123*, 1596–1601.

[19] L.-C. Song, C.-G. Li, J. Gao, B.-S. Yin, X. Luo, X.-G. Zhang, H.-L. Bao, Q.-M. Hu, *Inorg. Chem.* **2008**, *47*, 4545–4553.

[20] a) U.-P. Apfel, Y. Halpin, H. Görls, G. J. Vos, W. Weigand, *Eur. J. Inorg. Chem.* **2011**, 581–588; b) U.-P. Apfel, H. Görls, G. A. N. Felton, D. H. Evans, R. S. Glass, D. L. Lichtenberger, W. Weigand, *Helv. Chim. Acta* **2012**, *95*, 2168–2175.

[21] a) U.-P. Apfel, Y. Halpin, H. Görls, J. G. Vos, B. Schweizer, G. Linti, W. Weigand, *Chem. Biodivers.* **2007**, *4*, 2138–2148; b) P. I. Volkers, T. B. Rauchfuss, S. R. Wilson, *Eur. J. Inorg. Chem.* **2006**, 4793–4799.

[22] a) U.-P. Apfel, C. R. Kowol, Y. Halpin, F. Kloss, J. Kübel, H. Görls, J. G. Vos, B. K. Keppler, E. Morera, G. Lucente, W. Weigand, *J. Inorg. Biochem.* **2009**, *103*, 1236–1244; b) X. De Hatten, E. Bothe, K. Merz, I. Huc, N. Metzler-Nolte, *Eur. J. Inorg. Chem.* **2008**, 4530–4537; c) C. He, M. Wang, X. Zhang, Z. Wang, C. Chen, J. Liu, B. Åkermark, L. Sun, *Angew. Chem. Int. Ed.* **2004**, *43*, 3571–3574.

[23] E. J. Lyon, I. P. Georgakaki, J. H. Reibenspies, M. Y. Darensbourg, *J. Am. Chem. Soc.* **2001**, *123*, 3268–3278.

[24] a) D. Chong, I. P. Georgakaki, R. Mejia-Rodriguez, J. Sanabria-Chinchilla, M. P. Soriaga, M. Y. Darensbourg, *Dalton Trans.* **2003**, 4158–4163; b) E. J. Lyon, I. P. Georgakaki, J. H. Reibenspies, M. Y. Darensbourg, *Angew. Chem. Int. Ed.* **1999**, *38*, 3178–3180; c) X. Zhao, I. P. Georgakaki, M. L. Miller, R. Mejia-Rodriguez, C.-H. Chiang, M. Y. Darensbourg, *Inorg. Chem.* **2002**, *41*, 3917–3928; d) R. Mejia-Rodriguez, D. Chong, J. H. Reibenspies,

M. P. Soriaga, M. Y. Darensbourg, *J. Am. Chem. Soc.* **2004**, *126*, 12004–12014; e) J. W. Tye, J. Lee, H. W. Wang, R. Mejia-Rodriguez, J. H. Reibenspies, M. B. Hall, M. Y. Darensbourg, *Inorg. Chem.* **2005**, *44*, 5550–5552; f) S. J. Borg, T. Behrsing, S. P. Best, M. Razavet, X. Liu, C. J. Pickett, *J. Am. Chem. Soc.* **2004**, *126*, 16988–16999; g) A. Darchen, H. Mousser, H. Patin, *J. Chem. Soc., Chem. Commun.* **1988**, 968–970; b) H. Mousser, Ph. D. Thesis, University of Rennes, France, **1987**; h) F. Robin, R. Rumin, J. Talarmin, F. Y. Pétillon, K. W. Muir, *Organometallics* **1993**, *12*, 365–380; i) J.-F. Capon, S. Ezzaher, F. Gloaguen, F. Y. Pétillon, P. Schollhammer, J. Talarmin, T. J. Davin, J. E. McGrady, K. W. Muir, *New J. Chem.* **2007**, *31*, 2052–2064.

[25] D. Chong, I. P. Georgakaki, R. Mejia-Rodriguez, J. Sanabria-Chinchilla, M. P. Soriaga, M. Y. Darensbourg, *Dalton Trans.* **2003**, 4158–4163.

[26] a) J.-F. Capon, F. Gloaguen, P. Schollhammer, J. Talarmin, *J. Electroanal. Chem.* **2004**, *566*, 241–247; b) J. Windhager, M. Rudolph, S. Bräutigam, H. Görls, W. Weigand, *Eur. J. Inorg. Chem.* **2007**, 2748–2760.

[27] G. A. N. Felton, A. K. Vannucci, J. Chen, L. T. Lockett, N. Okumura, B. J. Petro, U. I. Zakai, D. H. Evans, R. S. Glass, D. L. Lichtenberger, *J. Am. Chem. Soc.* **2007**, *129*, 12521–12530.

[28] *COLLECT*, Data Collection Software; Nonius B. V., Netherlands, **1998**.

[29] "Processing of X-ray Diffraction Data Collected in Oscillation Mode"": Z. Otwinowski, W. Minor, in: *Methods in Enzymology, Vol. 276, Macromolecular Crystallography, Part A* (Eds.: C. W. Carter, R, M. Sweet), Academic Press **1997**, pp. 307–326.

[30] G. M. Sheldrick, *Acta Crystallogr., Sect. A* **2008**, *64*, 112–122.

Received: February 21, 2013
Published Online: April 11, 2013

Special Issue

